Mar Biotechnol (2015) 17:633–643
DOI 10.1007/s10126-015-9645-9

ORIGINAL ARTICLE

Intra-Colonial Functional Differentiation-Related Modulation of the Cellular Membrane in a Pocilloporid Coral *Seriatopora caliendrum*

Chuan-Ho Tang[1,2] · **Ping-Chang Ku**[3] · **Ching-Yu Lin**[4] · **Te-Hao Chen**[1,2] · **Kuo-Hsin Lee**[5] · **Shu-Hui Lee**[6] · **Wei-Hsien Wang**[1,3]

Received: 10 November 2014 / Accepted: 6 June 2015 / Published online: 5 August 2015

Abstract Scleractinian corals have displayed phenotypic gradients of polyps within a single genotypic colony, and this has profound implications for their biology. The intrinsic polymorphism of membrane lipids and the molecular interactions involved allow cells to dynamically organize their membranes to have physicochemical properties appropriate for their physiological requirements. To gain insight into the accommodation of the cellular membrane during ontogenetic shifts, intra-colony differences in the glycerophosphocholine profiling of a pocilloporid coral, *Seriatopora caliendrum*, were characterized using a previously validated method. Specifically, several major polyunsaturated phosphatidylcholines showed higher levels in the distal tissue of coral branches. In contrast, the corresponding molecules with 1–2-degree less unsaturation and plasmanylcholines were expressed more highly in the proximal tissue. The lipid profiles of these two colonial positions also contrasted sharply with regard to the saturated, monounsaturated, and lyso-glycerophosphocholine ratios. Based on the biochemical and biophysical properties of these lipids, the associated modulation of cellular membrane properties could be related to the physiological requirements, including coral growth and aging, of the functionally differentiated polyps. In this study, the metabolic regulation of membrane lipids involved in the functional differentiation of polyps within a *S. caliendrum* colony was identified.

Keywords Aging · Cellular performance · Growth · Molecular profiling · Oxidative stress · Phospholipid

Ping-Chang Ku contributed to this work as one of the first authors.

Electronic supplementary material The online version of this article (doi:10.1007/s10126-015-9645-9) contains supplementary material, which is available to authorized users.

✉ Chuan-Ho Tang
chtang@nmmba.gov.tw

✉ Wei-Hsien Wang
whw@mail.nsysu.edu.tw

[1] Department of Biology, National Museum of Marine Biology and Aquarium, 2 Houwan Rd., Checheng, Pingtung 944, Taiwan

[2] Institute of Marine Biology, National Dong Hwa University, Pingtung 944, Taiwan

[3] Department of Marine Biotechnology and Resources and Asia-Pacific Ocean Research Center, National Sun Yat-Sen University, 70 Lien-hai Rd, Kaohsiung 804, Taiwan

[4] Institute of Environmental Health, National Taiwan University, Taipei City 100, Taiwan

[5] Department of Emergency Medicine, E-Da Hospital, I-Shou University, Kaohsiung 824, Taiwan

[6] Central of General Education, National Kaohsiung Marine University, Kaohsiung 811, Taiwan

Introduction

Scleractinian corals, which provide the biogenic habitat for a variety of marine organisms, form the base of coral reef ecosystems. The ability of these corals to maintain and develop the framework of reefs is vital to the long-term persistence of ecosystem prosperity (Jones et al. 2004). In addition to recruitment, the shift in balance between the growth and decline of coral colonies is a critical process upon which the integrity of entire coral reef framework depends. In particular, branching corals, such as pocilloporids and acroporids, show large variations in this balance as a result of incorporating the properties of rapid degradation and regeneration into their colonies (Hall 1997). For example, a high potential for breakage appears in branching corals because their distal portions grow rapidly in length and number while they are exposed to mechanical

disturbances (Highsmith et al. 1980). In contrast to the distal portions, the tissue at the proximal regions of the coral branch appears more vulnerable and less vigorous, these parts are more aged and sensitive to mortality (Meesters and Bak 1995). The abundance of branching corals that are extremely susceptible to environmental variations has previously been attributed to this aging-related deterioration (Loya et al. 2001). The intra-colony arrangement in branching corals also shows sharp contrasts in energy metabolism, several physiobiochemical characteristics, and the correlated expression of genes involved in growth and resistance (Bay et al. 2009; D'Angelo et al. 2012; Fang et al. 1989; Gladfelter et al. 1989; Oku et al. 2002).

The stress response of scleractinian corals exposed to a variety of environmental insults, such as chemical, thermal, and irradiant stresses, strongly involves oxidative stress in the underlying etiology. As previously demonstrated, stressed corals induce a series of biochemical and physiological responses related to their oxidative circumstances, such as the overproduction of reactive oxygen species (ROS); the depletion of antioxidant capacity; the accumulation of oxidative damage molecules; and an increase in the expression of antioxidant enzymes, protein chaperons, and protein turnover activity (Baird et al. 2009; Downs et al. 2002; Lesser 2006). Oxidative stress places a burden on an organism through the excess generation and accumulation of ROS, such as superoxides and hydroxyl radicals, which cause cellular damage as the result of cellular abnormalities in energy conversion processes, including photosynthesis, catabolism, or anabolism (Lesser 2006; Murphy 2009). In addition to affecting exogenous insults, these toxic reactions appear to play major roles in various degenerative processes in the organisms, including illness and aging (Cadenas and Davies 2000). As has been revealed by extensive research, ROS can cause the oxidative modification of many cellular components, such as lipids, proteins, and DNA, resulting in decreased and inhibited cellular functioning, which can initiate the processes of cellular degradation (Avery 2011). In particular, lipid peroxidation can expand oxidative damage to the cellular membranes and is one of the vital challenges in the maintenance of cellular homeostasis. Under oxidative stress, membrane perturbations, including alterations in physical properties, modification of membrane protein activity, and permeabilization to nonspecific ions, such as Ca^{2+}, are causally linked to the occurrence of lipid peroxidation as an initiator of cellular degradation (Beranova et al. 2010; Stark 2005). Extensive lipid peroxidation ultimately disrupts membrane function and leads to the loss of cell viability.

Organisms that maintain their cellular functions by altering their membrane lipid and fatty acid compositions can remain viable even under extreme oxidative circumstances (Mykytczuka et al. 2011; Rozentsvet et al. 2012). Membrane lipids show a great diversity of molecular structures by varying the arrangement of chemical bonds that can accommodate the changes in the cellular membrane that occur due to an environmental disturbance or physiological senescence (Freikman et al. 2011; Tang et al. 2014a; Zehmer and Hazel 2005). The modified lipid structure can generate a membrane that has entirely different properties and thus exerts a potent effect on biological processes (Lee 2004; Vigh et al. 2005). Indeed, membrane lipids constitute the basic structural elements that create cellular membranes with the physicochemical properties appropriate for the physiological demands and that optimize cellular performance (van Meer et al. 2008). Even relatively small alterations in cellular membrane properties can elicit considerable changes in the efficiency of several membrane-dependent functions, leading to a chronic impairment in the fitness of organisms (Tang et al. 2014a). As a potential site of oxidative damage, the cellular membrane should be the focus of studies examining cellular stress and regulatory responses.

Most studies on coral membrane lipid composition have characterized the contradistinctions of many lipid classes and fatty acid content that were related to the different cellular physiological conditions both between and within colonies (Bachok et al. 2006; Yamashiro et al. 2001; Oku et al. 2002). These studies have provided insight into lipid metabolic responses, but they have been unable to reveal the relevance of these lipid shifts to the modulation of membrane properties and the related physiological requirements. Cellular functions must be coordinated with the appropriate membrane properties, which are largely determined by the ability of the lipid composition to adapt to the cellular situation. Therefore, to understand cellular function and regulation, it is essential to have insight into the molecular structures of altered membrane lipids. High-throughput methods in lipidomics have made this detailed analysis possible, allowing us to systematically conduct lipid profiling with an explicit description of the molecular structure. In this study, the membrane lipid profiles of a pocilloporid coral, *Seriatopora caliendrum*, were characterized according to the functional differentiations within the coral colony using a mass spectrometry-based lipidomics method. The lipid profiles revealed an interesting contrast between the distal and proximal portions of coral branches. The distinctions in lipid composition were related to the physiological requirements of coral growth and the cellular accommodation of aging-related physiological senescence to augment or maintain cellular functioning.

Materials and Methods

Coral Sample Collection

Considering the reproductive influence, coral sampling was done during the period when coral reproduction is inactive (Tang et al. 2014b). A branch was obtained during spring

2013 at depths of 8–10 m from each sample colony (15–20-cm diameter, $N=19$) of the pocilloporid coral *S. caliendrum* that inhabits the Houbibu region of Kenting National Park, Taiwan. The tip (0.1–0.5 cm from the branch end) and stalk (1–2 cm from the branch end) were collected, immediately frozen in liquid nitrogen, and stored at −80 °C. Based on a growth rate of approximately 4 cm/year (Edmunds 2005), the ages of the coral tip and stalk regions can be estimated to be 0.3–1.5 and 3–6 months old, respectively. The coral sampling was conducted under a permit issued by Kenting National Park Headquarters.

Identification of Zooxanthellae

Coral tissue was ground in liquid nitrogen and processed using a modified salting-out procedure for DNA extraction (Ferrara et al. 2006; Keshavmurthy et al. 2012). The coral sample was placed into 0.2 mL lysis buffer (0.25 M Tris, 2 % sodium dodecyl sulfate, 0.05 M EDTA at pH 8.0, and 0.1 M NaCl) with 4.0 μL proteinase K (25 mg/L) and lysed overnight at 55 °C. The lysed sample was carefully mixed with 0.2 mL saturated NaCl and centrifuged for 20 min at 10,000*g*. The supernatant was isolated and mixed with two volumes of 99.9 % cold ethanol and then stored at −20 °C for 30 min prior to centrifugation for 30 min at 12,000*g* (4 °C). The collected DNA pellet was washed three times with 99.9 % cold ethanol, dried by vacuum for 10 min, and then resuspended in sterile distilled water. To identify the clade of the zooxanthellae in the corals, nuclear large-subunit ribosomal DNA was amplified using the following host-excluding primers: forward 5S 5′-GCCGACCCGCTGAATTCAAGCATAT-3′ and reverse D23zoox 5′-TGTGGCAYGTGACGCGCAA GCTAAG-3′ (Chen et al. 2005). PCR analysis was conducted in 50-μL reaction volumes containing 10 μL 5× Excel *Taq* premix (SMOBIO Technology, Taiwan), 1 μL (10 pmol) of each primer, and 5 μL template DNA. The PCR reactions were carried out using a GeneAmp PCR System 2400 (Applied Biosystems, USA), and the conditions were as follows: an initial denaturation at 95 °C for 5 min; 30 cycles consisting of 95 °C for 30 s, 56 °C for 1 min, and 72 °C for 2 min; and the final elongation step at 72 °C for 6 min. Following PCR, the products were sequenced using an ABI 3730 DNA Analyzer (Applied Biosystems, USA), and the obtained sequences were searched for and aligned using the NCBI GenBank Database with BLAST (http://www.ncbi.nlm.nih.gov/).

Lipid Analysis

For lipid extraction, the frozen coral fractions were ground in a liquid nitrogen-cooled mortar and then lyophilized overnight (Tang et al. 2012). A three-replicate chemical measurement was conducted for each coral sample. The homogenous dry tissue was weighed and then extracted with a chloroform/methanol (2:1) solution. The mixture was then mixed thoroughly with a 0.15-M NaCl aqueous solution, and the complete lower layer was collected for further analysis. A validated high-performance liquid chromatography (HPLC)–tandem mass spectrometry method was used to profile the composition of glycerophosphocholines (GPCs) in the lipid extracts (Tang et al. 2012). Briefly, chromatographs of the lipid extracts were created with a reversed-phase gradient elution at a constant flow rate of 0.5 mL/min in an Agilent 1100 series HPLC system (Agilent Technologies, USA). The molecular information for the lipid species that emerged from the chromatographic column (Kinetex C_{18}, 2.6 μm, 100×2.1 mm; Phenomenex, USA) was acquired and recorded by a coupled API 4000 triple quadrupole mass spectrometer (Applied Biosystems, USA). An analytical strategy consisting of a two-stage tandem mass spectrometry experiment based on unique fragmentation patterns in the collision process was used to detail the GPC molecular species composition in the sample. The preliminary profile of GPCs in each sample was obtained using a precursor ion scan of *m*/*z* 184 (corresponding to the phosphorylcholine ion) in the positive mode, because this fragment signal is derived from the common feature of the molecular structure of GPCs. Subsequently, based on this phosphorylcholine-containing lipid profile, another tandem mass spectrometry experiment was conducted to acquire the product ion spectrum of each GPC species according to their respective elution times. The molecular structure of the GPC was then determined by illustrating the product ion spectra of the $[M+H]^+$, $[M+Na]^+$, $[M+Li]^+$, and $[M+Ac]^-$ ions.

Data Processing and Analysis

The acquired GPC profile data were processed using the software (Analyst 1.4; Applied Biosystems Instrument Co., USA) on the mass spectrometer. For the peak detection, each molecular mass ion signal was manually determined from a total ion chromatogram of pooled coral samples during a 0.2-min time window per step; the extracted peak was recorded as *m*/*z* and retention time. After removing duplicate peaks, the remaining peaks were checked again to remove latent isotope peaks. A quantitation method was created using the final peak list to quantify a batch of samples according to the Analyst 1.4 regulation procedure. Once a table of results was obtained, all the peaks in the batch were manually reviewed to confirm the accuracy of the peak alignment and the peak area integration. Ultimately, the peak list including the peak area of the extracted ion chromatogram was exported as a Microsoft Excel file for further analysis.

After the data were processed, each detected peak signal was normalized to the sum of the total signal response in the GPC profile. A principal components analysis (PCA) and an orthogonal partial least squares to latent

structures discriminant analysis (orthogonal partial least squares discriminant analysis (OPLS-DA)) were performed using SIMCA-P 13 statistical software (Umetrics AB, Umea, Sweden) to determine whether the metabolic differences in the GPC profiles from the coral tissues could be distinguished or modeled, respectively. PCA is a pattern recognition method that condenses the original set of variables into fewer variables based on their weighted averages; the new variables are called scores, and the weighted profiles are called loadings. Each GPC profile was represented as a data point in the score plot, and each point that was clustered together had a similar profile. The loading plot revealed information about the GPC molecular species that contributed to the data point separation observed in the score plot. Furthermore, the variations within and between groups can be separated using the OPLS-DA model, and this facilitates model interpretation. This supervised multivariate analysis method is useful for surveying the data and for recognizing the patterns of GPC profiles that are associated with specific sample groups. A one-way analysis of variance (ANOVA) was used to further assess the significant differences ($p<0.05$) of the sifted GPC molecular species obtained from the coral tissues at the tip and stalk positions.

Lipid Nomenclature

GPCs are composed of a glycerol backbone with a phosphorylcholine head group at the *sn*-3 position and a fatty acid substituent at the *sn*-1 and *sn*-2 positions. The fatty acid substituent can be linked via an ester at both positions, and long-chain alkyl ether or vinyl ether linkages can also be adopted at the *sn*-1 position. Because of the differences in linkages at the *sn*-1 position, GPCs are further divided into phosphatidylcholine (1,2-diacyl-GPC), plasmanylcholine (1-O-alkyl-2-acyl-GPC), and plasmenylcholine (1-O-alk-1′-enyl-2-acyl-GPC) subclasses. The designations and abbreviations for GPC molecular species are based on the recommendations of the Lipid Metabolites and Pathways Strategy (LIPID MAPS). For example, 1,2-dihexadecanoyl-, 1-hexadecyl-2-hexadecanoyl-, and 1-(1Z-hexadecenyl)-2-hexadecanoyl-*sn*-glycero-3-phosphocholine are abbreviated as PC(16:0/16:0), PC(O-16:0/16:0), and PC(P-16:0/16:0), respectively; the molecular structures for these lipids are shown in Fig. 1. The notation x:y for a fatty acid chain indicates the number of carbon atoms (x) and double bonds (y). Additionally, symbols marked with "O" or "P" indicate a fatty acid chain linkage with the glycerol backbone via an alkyl or vinyl ether, respectively, generally at the *sn*-1 position; no marks indicate an ester linkage. In cases where both fatty acid chains cannot be assigned, the sum of their carbon atom and double-bond numbers can be derived from the deductive inference of the molecule once the lipid subclass is identified. These lipids are correspondingly abbreviated PC(32:0), PC(O-32:0), and PC(P-32:0). Molecular species of GPCs that possess a hydroxyl substituent at either the *sn*-1 or the *sn*-2 position of the glycerol backbone are named lyso-GPC; for example, 1-hexadecanoyl-2-hydroxyl-*sn*-glycero-3-phosphocholines can be abbreviated as PC(16:0/0:0).

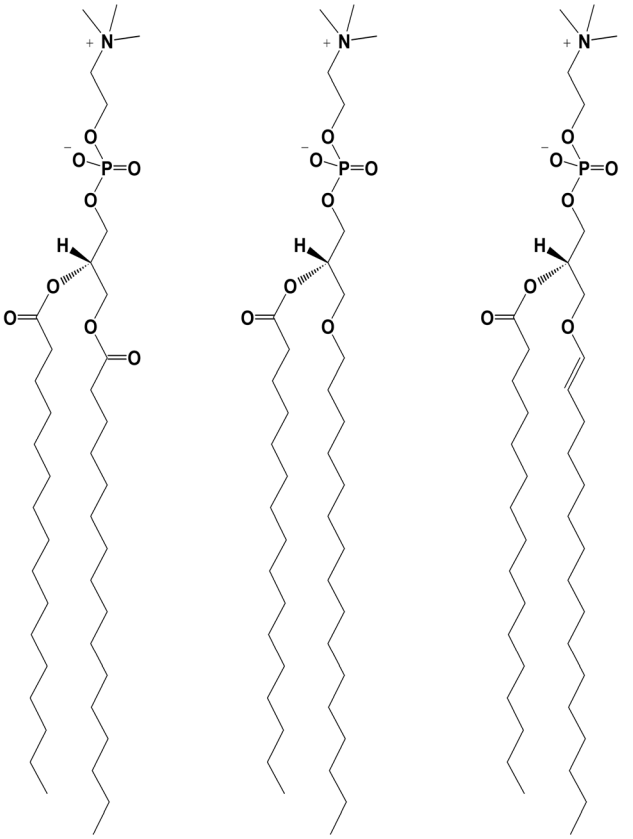

Fig. 1 Structure of three glycerophosphocholine subclasses. PC(16:0/16:0), PC(O-16:0/16:0), and PC(P-16:0/16:0) are indicated for 1,2-dihexadecanoyl-, 1-hexadecyl-2-hexadecanoyl-, and 1-(1Z-hexadecenyl)-2-hexadecanoyl-*sn*-glycero-3-phosphocholine, respectively

Results

Of the 187 signal peaks detected in the GPC profile of *S. caliendrum*, 144 identified molecular species are listed in Table 1 along with a ratio accounting for the GPC composition in the coral tissues at both the tip and stalk positions. The identification of the zooxanthellae (accession: KM287430) indicated a high similarity to the sequence belonging to clade C, which ensures a strong specificity for the lipid composition in the coral samples. Therefore, the result should be

Table 1 The glycerophosphocholine molecular species identified in the coral (*Seriatopora caliendrum*) tissue in the tip and stalk portions

Lipid\position	Percentage (%)[a] Tip	Stalk	Lipid\position	Percentage (%) Tip	Stalk
Lyso-glycerophosphocholine					
PC(0:0/16:0)	0.005±0.002	0.005±0.003	PC(0:0/22:5)*	0.015±0.009	0.006±0.004
PC(0:0/18:0)	0.003±0.001	0.003±0.002	PC(0:0/22:6)*	0.099±0.030	0.022±0.008
PC(0:0/18:1)+	0.006±0.002	0.002±0.001	PC(16:0/0:0)*	0.140±0.057	0.049±0.019
PC(18:1/0:0)[b]*			PC(18:0/0:0)*	0.082±0.034	0.046±0.012
PC(0:0/18:2)+	0.006±0.002	0.001±0.001	PC(20:2/0:0)*	0.001±0.001	<0.001±0.000
PC(18:2/0:0)[b]*			PC(20:3/0:0)*	0.002±0.001	0.001±0.001
PC(0:0/18:3)+	0.009±0.004	0.001±0.001	PC(20:4/0:0)*	0.004±0.002	0.002±0.001
PC(18:3/0:0)[b]*			PC(22:4/0:0)	0.002±0.001	0.001±0.001
PC(0:0/20:2)*	0.006±0.003	0.002±0.001	PC(22:5/0:0)*	0.004±0.002	0.002±0.004
PC(0:0/20:3)*	0.012±0.006	0.003±0.003	PC(22:6/0:0)*	0.020±0.008	0.007±0.003
PC(0:0/20:4)*	0.023±0.007	0.006±0.003	PC(23:6/0:0)*	0.004±0.001	0.003±0.001
PC(0:0/20:5)+	0.012±0.007	0.002±0.002	PC(O-16:0/0:0)*	0.055±0.011	0.027±0.010
PC(20:5/0:0)[b]*			PC(O-16:1/0:0)*	0.016±0.007	0.006±0.003
PC(0:0/21:6)+	0.009±0.004	0.003±0.002	PC(O-17:0/0:0)*	0.004±0.002	0.002±0.001
PC(21:6/0:0)[b]*			PC(O-18:0/0:0)*	0.108±0.045	0.072±0.014
PC(0:0/22:4)*	0.019±0.009	0.005±0.003			
Phosphatidylcholine					
PC(14:0/14:0)	0.013±0.013	0.012±0.009	PC(18:0/20:5)*	0.853±0.130	0.862±0.177
PC(16:0/14:0)	0.106±0.040	0.133±0.077	PC(18:0/22:3)	0.040±0.011	0.041±0.012
PC(16:0/16:0)	0.035±0.015	0.051±0.036	PC(18:0/22:4)*	0.094±0.018	0.098±0.016
PC(16:0/16:1)	0.102±0.013	0.115±0.041	PC(18:0/22:5)	0.461±0.098	0.608±0.177
PC(16:0/18:1)*	0.324±0.063	0.536±0.253	PC(18:0/22:6)	2.011±0.183	1.836±0.212
PC(16:0/18:2)	0.847±0.141	0.776±0.138	PC(18:0/24:5)*	0.136±0.023	0.128±0.012
PC(16:0/18:3)*	1.265±0.159	1.051±0.178	PC(18:0/24:6)	0.024±0.006	0.026±0.004
PC(16:0/18:5)*	0.022±0.006	0.018±0.004	PC(18:1/22:6)	0.094±0.013	0.095±0.014
PC(16:0/20:3)+	2.040±0.241	2.073±0.258	PC(20:0/20:4)*	0.625±0.077	0.630±0.074
PC(18:0/18:3)[b]			PC(20:0/22:4)*	0.033±0.007	0.035±0.005
PC(16:0/20:4)*	4.231±0.520	3.676±0.398	PC(20:0/22:6)*	0.064±0.012	0.052±0.006
PC(16:0/20:5)	1.874±0.220	1.812±0.291	PC(20:0/24:5)	0.011±0.003	0.010±0.002
PC(16:0/22:3)	0.506±0.068	0.562±0.071	PC(20:1/20:1)	0.091±0.023	0.110±0.017
PC(16:0/22:4)	0.867±0.126	1.017±0.265	PC(22:1/16:0)	0.009±0.004	0.012±0.005
PC(16:0/22:5)	1.601±0.348	2.248±0.939	PC(22:6/22:6)	0.244±0.086	0.193±0.086
PC(16:0/22:6)*	10.324±0.767	9.765±0.755	PC(27:0)*	0.007±0.003	0.010±0.003
PC(16:0/24:6)*	0.079±0.014	0.076±0.011	PC(32:2)	0.011±0.002	0.012±0.003
PC(16:1/16:1)	0.018±0.005	0.016±0.005	PC(33:1)	0.015±0.002	0.016±0.005
PC(16:1/16:2)	0.016±0.004	0.015±0.003	PC(34:0)*	0.008±0.003	0.012±0.006
PC(16:1/16:3)	0.007±0.003	0.007±0.001	PC(35:1)*	0.013±0.002	0.016±0.004
PC(16:1/18:3)	0.559±0.107	0.507±0.104	PC(36:4)	0.338±0.094	0.320±0.045
PC(16:1/22:6)	0.028±0.007	0.022±0.006	PC(36:6)	0.161±0.047	0.170±0.039
PC(16:2/18:3)	0.019±0.005	0.022±0.008	PC(37:0)*	0.030±0.011	0.033±0.010
PC(17:0/22:6)	0.156±0.029	0.129±0.024	PC(38:1)*	0.013±0.004	0.014±0.004
PC(18:0/18:1)*	0.162±0.027	0.205±0.056	PC(41:4)*	0.019±0.004	0.018±0.004
PC(18:0/18:2)+	0.791±0.129	0.834±0.119	PC(41:6)	0.021±0.004	0.019±0.004
PC(16:0/20:2)[b]			PC(42:3)*	0.033±0.008	0.025±0.006
PC(18:0/20:2)	0.193±0.051	0.181±0.047	PC(43:4)*	0.022±0.005	0.017±0.006
PC(18:0/20:4)*	1.335±0.226	1.346±0.163			

Table 1 (continued)

Lipid\position	Percentage (%)[a] Tip	Stalk	Lipid\position	Percentage (%) Tip	Stalk
Plasmanylcholine					
PC(O-14:0/20:4)*	0.196±0.024	0.179±0.019	PC(O-18:0/20:3)*	1.078±0.196	1.303±0.206
PC(O-14:2/25:3)*	0.024±0.016	0.041±0.027	PC(O-18:0/20:4)*	15.351±1.284	14.459±1.169
PC(O-15:2/16:0)	0.064±0.019	0.055±0.025	PC(O-18:0/20:5)	3.155±0.499	3.434±0.487
PC(O-16:0/14:0)*	0.156±0.048	0.313±0.107	PC(O-18:0/22:4)	0.258±0.026	0.283±0.057
PC(O-16:0/16:0)*	0.096±0.037	0.167±0.060	PC(O-18:0/22:5)	0.237±0.062	0.295±0.076
PC(O-16:0/18:1)*	0.201±0.054	0.295±0.076	PC(O-18:0/22:6)*	1.246±0.183	1.440±0.280
PC(O-16:0/18:2)*	0.212±0.037	0.265±0.032	PC(O-19:0/16:1)*	0.033±0.009	0.040±0.010
PC(O-16:0/18:3)	0.318±0.063	0.346±0.068	PC(O-19:0/20:4)*	0.286±0.041	0.248±0.028
PC(O-16:0/20:2)	0.316±0.054	0.319±0.045	PC(O-19:0/20:5)*	0.083±0.009	0.089±0.016
PC(O-16:0/20:3)*	1.197±0.183	1.872±0.206	PC(O-20:0/16:1)*	0.106±0.033	0.135±0.039
PC(O-16:0/20:4)	14.347±1.300	14.581±1.152	PC(O-20:0/18:1)	0.009±0.002	0.009±0.003
PC(O-16:0/22:4)*	0.200±0.034	0.279±0.056	PC(O-20:1/20:3)	0.103±0.019	0.116±0.023
PC(O-16:0/22:6)	3.077±0.490	3.310±0.361	PC(O-20:2/20:4)*	0.031±0.006	0.030±0.008
PC(O-16:0/24:5)*	0.092±0.015	0.113±0.022	PC(O-31:2)	0.013±0.004	0.012±0.003
PC(O-16:1/14:0)	0.357±0.118	0.404±0.120	PC(O-32:6)	0.011±0.002	0.010±0.002
PC(O-16:1/16:0)*	0.150±0.032	0.204±0.047	PC(O-36:6)	0.048±0.014	0.046±0.015
PC(O-16:1/20:4)+	13.958±1.032	12.473±1.452	PC(O-37:6)	0.082±0.034	0.091±0.038
PC(O-16:0/20:5)[b]*			PC(O-38:5)*	0.588±0.110	0.817±0.211
PC(O-16:1/20:5)*	1.664±0.284	1.318±0.178	PC(O-39:0)*	0.027±0.003	0.028±0.004
PC(O-17:0/20:4)	0.706±0.080	0.746±0.095	PC(O-39:3)	0.056±0.012	0.086±0.020
PC(O-17:1/22:4)*	0.026±0.005	0.040±0.009	PC(O-42:4)	0.008±0.004	0.005±0.002
PC(O-18:0/16:0)	0.036±0.009	0.041±0.012			
Plasmenylcholine					
PC(P-14:1/20:3)	0.052±0.007	0.051±0.010	PC(P-34:4)	0.036±0.008	0.038±0.012
PC(P-15:0/22:4)	0.304±0.047	0.302±0.061	PC(P-38:1)	0.086±0.024	0.096±0.022
PC(P-16:0/22:6)	0.465±0.090	0.424±0.081	PC(P-39:0)	0.044±0.009	0.052±0.012
PC(P-17:0/20:4)	0.208±0.128	0.265±0.186	PC(P-42:2)	0.039±0.007	0.053±0.010
PC(P-17:1/18:2)	0.077±0.015	0.070±0.010	PC(P-42:5)	0.054±0.011	0.051±0.008
PC(P-18:0/20:4)	0.182±0.030	0.198±0.048	PC(P-43:1)	0.032±0.006	0.039±0.006
PC(P-18:2/22:4)	0.036±0.008	0.050±0.019			

*Significant difference (ANOVA, $p<0.05$) of the lipid percentage in the coral tissue between the tip and stalk positions

[a] Percentage is a mean of the relative signal intensity in relation to the total signal response of lipids in the coral tissues (mean±standard deviation, $n=19$)

[b] The percentage was contained as the isobaric molecular species

considered as evidence that the coral *S. caliendrum* harbors the specific zooxanthellae identified in this study. The analysis revealed that a few of the molecular species including PC(16:0/22:6), PC(O-16:0/20:4), PC(O-16:1/20:4), PC(O-16:0/20:5), and PC(O-18:0/20:4) accounted for more than 50 % of the GPC composition in the coral. Approximately 60 % of the GPC composition in the tissues of *S. caliendrum* was composed of plasmanylcholine molecular species. The other GPC subclass, phosphatidylcholine and plasmanylcholine, accounted for approximately 30 and 1.6 % of the GPC composition, respectively. In terms of total proportions, there are no clear differences in these three GPC subclasses between the coral tissues at the tip and stalk positions. Nevertheless, the total proportion of lyso-GPCs (lyso-phosphatidylcholines and lyso-plasmanylcholines) in the tissues from the coral tip (0.669 %) was significantly higher (ANOVA, $p<0.05$) than that from the stalk (0.279 %).

The differences in the phosphorylcholine-containing lipid profiles between the coral samples were visualized in a PCA score plot. As shown in Fig. 2a, the cluster of data points belonging to different groups is clearly divided, distinguishing the coral tissues from the tip and stalk positions from each other based on the differences in their

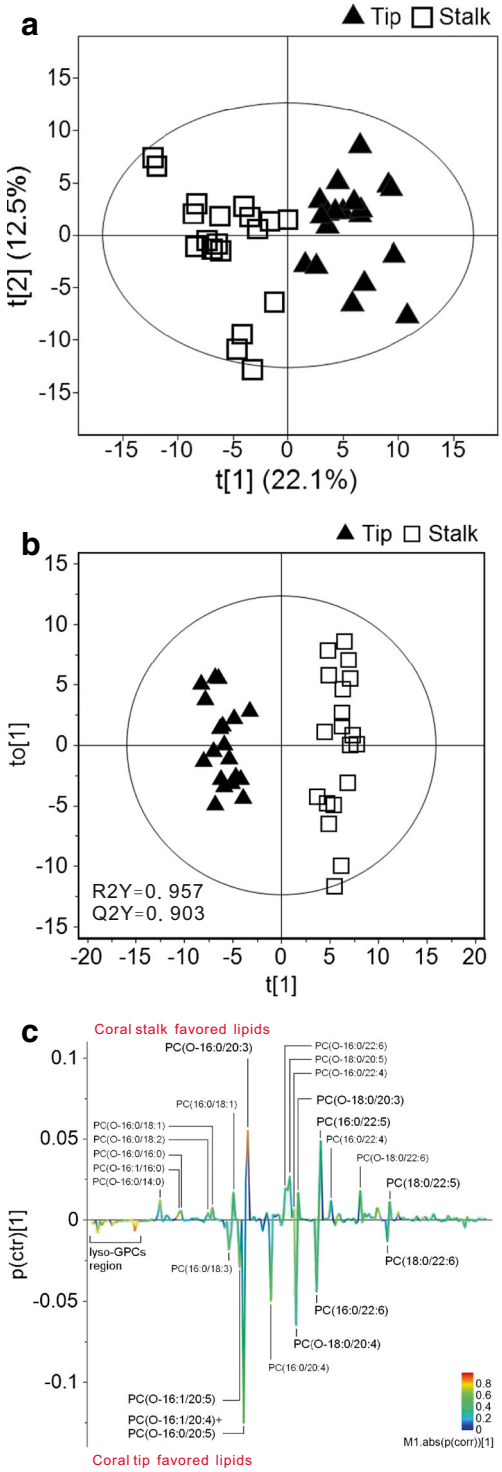

◀ **Fig. 2** Glycerophosphocholine profile analysis of coral tissues. **a** The score plots of the principal components analysis (PCA) and **b** the orthogonal partial least squares to latent structures discriminant analysis (OPLS-DA), which show a distinguishable separation between the tip and stalk tissues of the coral (*Seriatopora caliendrum*). In the PCA score plot, the first principal component (t[1]) describes a variation of 22.1 % that contributes to the group separation. The OPLS-DA model resulted in one predictive (t[1]) and one orthogonal (to[1]) component, with a goodness-of-fit of R2Y=0.957 and cross-validated predictive abilities of Q2Y=0.903. **c** The S-line plot of the OPLS-DA model showing the glycerophosphocholine differences responsible for the discrimination between the coral tip and stalk tissues. The S-line plot visualizes the modeled covariation (p(ctr) [1] as a magnitude eigenvalue directed toward the coral stalk), colored according to the modulus of the modeled correlation (p(corr) [1], representing the reliability)

GPC profiles. The first principal component that contributed to the group separation in the score plot described a variation of 22.1 %. The covariance and correlation loading plots that revealed discriminatory GPC signal peaks are shown in Fig. S1 (in the electronic supplementary material). The coral GPC profiles of the tip and stalk groups were further modeled by OPLS-DA, as shown in Fig. 2b. The model resulted in one predictive and one orthogonal components (1+1) with a goodness-of-fit of R2Y=0.957 and cross-validated predictive abilities of Q2Y=0.903. The contrast in the lipid profiles between the two groups is presented in an S-line plot where the key features can be directly observed. As shown in Fig. 2c, distinct ratios of saturated, monounsaturated, and lyso- GPC are highlighted by high levels of correlation despite their small weights. In addition, there is a key difference showing the favoring of the two coral positions by polyunsaturated GPCs with unsaturation levels that differ by one or two degrees. As shown, the covariance direction of PC(16:0/22:6), PC(18:0/22:6), PC(O-16:0/20:5), and PC(O-18:0/20:4) is opposite to that of PC(16:0/22:5), PC(18:0/22:5), PC(O-16:0/20:3), and PC(O-18:0/20:3), and such lipid species accounted for the majority of the weighting to distinguish between the two lipid profiles of the coral tissues. Likewise, the phosphatidylcholine species PC(16:0/22:6) and PC(18:0/22:6) also showed a covariance that contrasts with their corresponding plasmanylcholine species PC(O-16:0/22:6) and PC(O-18:0/22:6), which allowed us to differentiate between the lipid profiles.

The GPC species with significant differences (ANOVA, $p<0.05$) in the ratio between the tip and stalk positions of the coral tissue are shown in Fig. 3. The primary feature of tissue from the coral tip was a greater proportion of lyso-GPCs; the ratio of the 28 molecules was 51–581 % greater than in the stalk tissue. In contrast, the ratio of seven phosphatidylcholines and seven plasmanylcholines that are either saturated or monounsaturated was 0.5–50 % higher in the stalk tissue than in the tip tissue. There were ten molecular species of polyunsaturated plasmanylcholines that showed greater proportions in the stalk tissue, while the seven other species that possess a 20-carbon chain that is unsaturated by 4–5 degrees, including three predominant GPC species, were more highly expressed in the tip tissues. Similarly, ten polyunsaturated phosphatidylcholines, including two predominant GPC

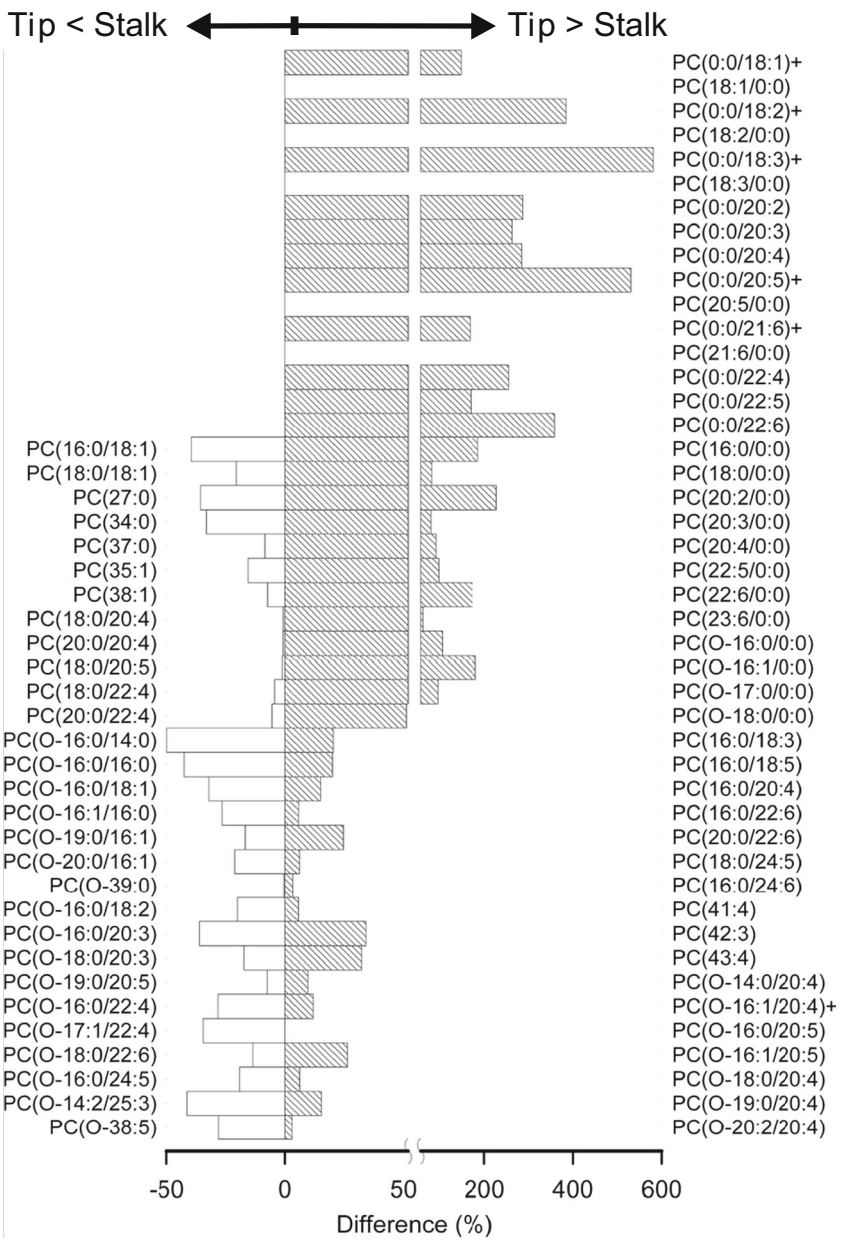

Fig. 3 Significant differences in lipid species between the coral tip and stalk tissues. The difference in the proportion of glycerophosphocholine (ANOVA, $p<0.05$) in *Seriatopora caliendrum* tissue from the tip portion compared to the stalk portion

species, showed a greater proportion in the tip tissue, while five others showed greater ratios in the stalk tissue.

Discussion

Differences in Growth Rate Between the Coral Tip and Stalk

Among diverse coral forms, branching corals have been known to develop the most separation of function within colonies (Soong and Lang 1992). One of the most visible examples of this is that the coral branch grows faster at the distal position compared to the proximal portion (Elahi and Edmunds 2007). The higher levels of lyso-GPCs and polyunsaturated GPCs in the tip likely reflect the cellular physiology requirements for rapid coral growth. In particular, the majority of the favored plasmanylcholines in the tip tissue possessed arachidonic acid (20:4), and the polyunsaturated GPCs in those tissues tended to be more unsaturated.

Scleractinian coral growth involves the formation of a great quantity of skeleton that requires the transport of many materials through calicoblastic cells (Tambutte et al. 2011). Transporting calcium through calicoblastic cells into the underlying space is one of the fundamental actions during the process of coral calcification. By

directly altering membrane characteristics, lyso-GPCs can increase the activity of L-type calcium ion channels and calcium ATPase and thus enhance calcium ion currents (Grosman 2001; Kraichely et al. 2009). Lyso-GPCs also potentiate the activation of protein kinases that can phosphorylate calcium ATPase, calcium channels, and their regulatory proteins to stimulate calcium ion flux activity (Edes and Kranias 2001; Sasaki et al. 1993; Shier et al. 1976). Another cellular action that is required for coral calcification is the vesicle-mediated secretion of "organic matrix" from calicoblastic cells (Clode and Marshall 2002). During this process, calicoblastic cells are extensively involved in membrane vesiculation and fusion, where the membrane adopts a highly curved architecture. The inverted cone molecular shape of lyso-GPCs allows the membrane to construct a positive curvature during vesiculation (Fuller and Rand 2001). In the membrane fusion process, saturated lyso-GPCs can induce a fully interdigitated membrane structure that enlarges the surface area and diminishes inter-membrane repulsion, which facilitates membrane contact prior to the merging step (Komatsu and Okada 1995; Lu et al. 2001). The increase in polyunsaturated phosphatidylcholines in the contacted membranes facilitates the formation of the inverted hexagonal phase and promotes the mixing of lipids during the membrane-merging step (Chernomordik and Kozlov 2008; Szule et al. 2002). Moreover, polyunsaturated phosphatidylcholines facilitate the membrane dynamics involved in organizing lipid rafts, which is an important factor in the initiation of membrane fusion (Baenziger et al. 1992; Lingwood and Simons 2010).

In addition to skeleton formation, coral growth involves cell growth that must fit the appropriate conditions of cellular physiology. Plasmanylcholine levels have been shown to positively correlate with accelerated cell growth and the levels of cellular differentiation (Albert and Anderson 1977; Chabot et al. 1990). Under conditions of cell growth, an abundance of arachidonic acid is also required for the production of eicosanoids (Sellmayer et al. 1996). Concurrently, higher levels of plasmanylcholines possessing arachidonic acid in the coral tips are also required for cellular growth. In addition, the regulation of desaturases that are involved in the modulation of cellular growth results in differences in the ratio of polyunsaturated GPCs with dissimilar unsaturation between the tips and stalks of the coral (Kates and Paradis 1973). Enhanced lyso-GPC production results in a state of accelerated cell growth (Okita et al. 1997), which is also found in the coral tip tissues relative to the stalk tissues. This metabolic distinction in lyso-GPC production is consistent with the variations in gene expression that are associated with lysosome lipase activity in coral cells (Bay et al. 2009).

Aging Gradient of Coral Polyps from the Distal to Proximal Region

In contrast to the coral tip, coral stalk tissue appears less vigorous and exhibits a reduced capability for growth and regeneration that is related to the aging of polyps (Meesters and Bak 1995). As previously reported for other organisms, the accrual of oxidative stress has been postulated to be responsible for the physiological senescence of coral polyps during the aging process (Sohal and Orr 2012). Additionally, in natural habitats, there are various environmental parameters that cyclically augment the physiological burdens of coral, such as photosynthesis-derived oxidative stress (Mayfield et al. 2010; Yellowlees et al. 2008). Once oxidative stress is enhanced to challenge the remaining anti-oxidant capacity, the cells in older coral polyps likely become more vulnerable. Membrane permeabilization has been established to be one of the underlying mechanisms that cause functional cell losses following oxidative insults that result in a decrease in molecular membrane density (Smith et al. 2009). Therefore, it is vital for the coral cells to safeguard the membrane from oxidative damage, permeabilization, and subsequent cell/organelle swelling-induced tension stress (Trump and Berezesky 1996). At the coral stalk, the older polyps appeared to decrease their lyso-GPC levels, exchange polyunsaturated phosphatidylcholines for corresponding species of plasmanylcholines, adopt higher levels of saturated and monounsaturated GPCs, and down-regulate the desaturation of GPCs. The shift in these lipids provides clues about the requirements for cellular accommodation to oxidative conditions for the purposes of maintaining the barrier property and structural integrity of the membrane.

Oxidative degradation leads to the formation of membrane pores as a result of the rebalancing of molecular interactions facilitated by the geometric packing of a specific molecule, such as lyso-GPCs (Hull et al. 2004; Smith et al. 2009). Therefore, a decrease in the levels of lyso-GPCs in the stalk plays a beneficial role in keeping coral cells from forming membrane pores, which helps to avoid effective permeabilization derived from the increase in oxidative stress. The exchange of polyunsaturated phosphatidylcholines for corresponding plasmanylcholines and the increase in saturated and monounsaturated plasmanylcholines are also beneficial to the cells of coral stalk in maintaining the properties of the membrane barrier. Due to the replacement of the carbonyl group with a methylene, plasmanylcholines can enhance the membrane barriers against ion and water permeability, regulating the oxidative assault-caused decrease of molecular membrane density (Chen and Gross 1994; Pandey and Roy 2011). The increase in monounsaturated GPCs can strengthen the mechanical stability of the membrane, allowing it to resist tension-induced leakage due to cell/organelle swelling when cells suffer from potent oxidative damage (Shoemaker and Vanderlick

2002). The decrease in lyso-GPCs minimizes the elastic free energy of the membrane during cell/organelle swelling and thus maintains architectural stability (Fuller and Rand 2001).

Polyunsaturated phosphatidylcholines are most likely to be the targets of oxidative stress due to their effects on membrane permeability and their highly reactive properties (Olbrich et al. 2000; Ollila et al. 2007). By exchanging polyunsaturated phosphatidylcholines for the corresponding plasmanylcholines, the stalk cells can further alleviate lipid oxidation by decreasing access to the polyunsaturated chain. Similarly, lowering the degree of fatty acid chain unsaturation is a protective mechanism against aging-related oxidative damage through the decrease in sensitivity to peroxidation (Pamplona et al. 2002). Saturated and monounsaturated GPCs have also been shown to increase membrane density and to be resistant to oxidative attack (Rozentsvet et al. 2012; Smith et al. 2009). Through such lipid modulation, coral cells could solidify their membrane rigidity to safeguard against oxidative degradation. As found in previous studies, a higher ratio of saturated and monounsaturated chains accompanying a lower level of polyunsaturated chains is adopted in coral polyps with relatively weak cellular physiology (Bachok et al. 2006; Yamashiro et al. 2001). Clearly, retarding oxidative progress is important for accommodating the cellular membrane in response to oxidative conditions.

In the present study, the metabolic differentiation of membrane lipid within a *S. caliendrum* colony was related to the physiological requirements for growth and cellular accommodation and to the oxidative effects accrued by aging. The coral cells compulsorily shifted their membrane lipid compositions during the aging process, accommodating the oxidative situation at the cost of vitality. Indeed, the shift in lipid composition includes several important signaling molecules, such as lyso-GPCs and polyunsaturated fatty acid chains, which govern basic cellular activities and actions (Meyer zu Heringdorf and Jakobs 2007). Therefore, this intra-colony shift in lipid metabolism is also likely to compromise cellular performance and ultimately lead to physiological senescence.

Acknowledgments The research was supported by the Ministry of Science & Technology (MOST 104-2221-E-291-001), National Museum of Marine Biology & Aquarium and National Dong Hwa University in Taiwan.

References

Albert DH, Anderson CE (1977) Ether-linked glycerolipids in human-brain tumors. Lipids 12:188–192

Avery SV (2011) Molecular targets of oxidative stress. Biochem J 434: 201–210

Bachok Z, Mfilinge P, Tsuchiya M (2006) Characterization of fatty acid composition in healthy and bleached corals from Okinawa, Japan. Coral Reefs 25:545–554

Baenziger JE, Jarrell HC, Smith CP (1992) Molecular motions and dynamics of a diunsaturated acyl chain in a lipid bilayer: implications for the role of polyunsaturation in biological membranes. Biochemistry 31:3377–3385

Baird AH, Bhagooli R, Ralph PJ, Takahashi S (2009) Coral bleaching: the role of the host. Trends Ecol Evol 24:16–20

Bay LK, Nielsen HB, Jarmer H, Seneca F, van Oppen MJH (2009) Transcriptomic variation in a coral reveals pathways of clonal organization. Mar Genomics 2:119–125

Beranova L, Cwiklik L, Jurkiewicz P, Hof M, Jungwirth P (2010) Oxidation changes physical properties of phospholipid bilayers: fluorescence spectroscopy and molecular simulations. Langmuir 26:6140–6144

Cadenas E, Davies KJA (2000) Mitochondrial free radical generation, oxidative stress, and aging. Free Radic Biol Med 29:222–230

Chabot MC, Greene DG, Brockschmidt JK, Capizzi RL, Wykle RL (1990) Ether-linked phosphoglyceride content of human leukemia cells. Cancer Res 50:7174–7178

Chen CA, Yang YW, Wei NV, Tsai WS, Fang LS (2005) Symbiont diversity in scleractinian corals from tropical reefs and subtropical non-reef communities in Taiwan. Coral Reefs 24:11–22

Chen X, Gross RW (1994) Phospholipid subclass-specific alterations in the kinetics of ion transport across biologic membranes. Biochemistry 33:13769–13774

Chernomordik LV, Kozlov MM (2008) Mechanics of membrane fusion. Nat Struct Mol Biol 15:675–683

Clode PL, Marshall AT (2002) Low temperature X-ray microanalysis of calcium in a scleractinian coral: evidence of active transport mechanisms. J Exp Biol 205:3543–3552

D'Angelo C, Smith EG, Oswald F, Burt J, Tchernov D, Wiedenmann J (2012) Locally accelerated growth is part of the innate immune response and repair mechanisms in reef-building corals as detected by green fluorescent protein (GFP)-like pigments. Coral Reefs 31: 1045–1056

Downs CA, Fauth JE, Halas JC, Dustan P, Bemiss J, Woodley CM (2002) Oxidative stress and seasonal coral bleaching. Free Radic Biol Med 33:533–543

Edes I, Kranias EG (2001) Ca^{2+}-ATPases. In: Sperelakis N (ed) Cell physiology source book. Academic Press, San Diego, pp 271–282

Edmunds PJ (2005) The effect of sub-lethal increases in temperature on the growth and population trajectories of three scleractinian corals on the southern Great Barrier Reef. Oecologia 140:350–364

Elahi R, Edmunds PJ (2007) Tissue age affects calcification in the scleractinian coral *Madracis mirabilis*. Biol Bull 212:20–28

Fang LS, Chen YWJ, Chen CS (1989) Why does the white tip of stony coral grow so fast without zooxanthellae? Mar Biol 103:359–363

Ferrara GB, Murgia B, Parodi AM, Valisano L, Cerrano C, Palmisano G, Bavestrello G, Sara M (2006) The assessment of DNA from marine organisms via a modified salting-out protocol. Cell Mol Biol Lett 11:155–160

Freikman I, Ringel I, Fibach E (2011) Oxidative stress-induced membrane shedding from RBCs is Ca flux-mediated and affects membrane lipid composition. J Membr Biol 240:73–82

Fuller N, Rand RP (2001) The influence of lysolipids on the spontaneous curvature and bending elasticity of phospholipid membranes. Biophys J 81:243–254

Gladfelter EH, Michel G, Sanfelici A (1989) Metabolic gradients along a branch of the reef coral *Acropora palmata*. Bull Mar Sci 44:1166–1173

Grosman N (2001) Similar effects of ether phospholipids, PAF and lyso-PAF on the Ca^{2+}-ATPase activity of rat brain synaptosomes and leukocyte membranes. Int Immunopharmacol 1:1321–1329

Hall VR (1997) Interspecific differences in the regeneration of artificial injuries on scleractinian corals. J Exp Mar Biol Ecol 121:9–23

Highsmith RC, Riggs AC, D'Antonio CM (1980) Survival of hurricane-generated coral fragments and a disturbance model of reef calcification/growth rates. Oecologia 46:322–329

Hull MC, Sauer DB, Hovis JS (2004) Influence of lipid chemistry on the osmotic response of cell membranes: effect of non-bilayer forming lipids. J Phys Chem B 108:15890–15895

Jones GP, McCormick MI, Srinivasan M, Eagle JV (2004) Coral decline threatens fish biodiversity in marine reserves. Proc Natl Acad Sci U S A 101:8251–8253

Kates M, Paradis M (1973) Phospholipid desaturation in *Candida lipolytica* as a function of temperature and growth. Can J Biochem 51:184–197

Keshavmurthy S, Hsu CM, Kuo CY, Meng PJ, Wang JT, Chen CA (2012) Symbiont communities and host genetic structure of the brain coral *Platygyra verweyi*, at the outlet of a nuclear power plant and adjacent areas. Mol Ecol 21:4393–4407

Komatsu H, Okada S (1995) Ethanol-induced aggregation and fusion of small phosphatidylcholine liposome: participation of interdigitated membrane formation in their processes. Biochim Biophys Acta 1235:270–280

Kraichely RE, Strege PR, Sarr MG, Kendrick ML, Farrugia G (2009) Lysophosphatidyl choline modulates mechanosensitive L-type Ca^{2+} current in circular smooth muscle cells from human jejunum. Am J Physiol Gastrointest Liver Physiol 296:G833–G839

Lee AG (2004) How lipids affect the activities of integral membrane proteins. Biochim Biophys Acta 1666:62–87

Lesser MP (2006) Oxidative stress in marine environments: biochemistry and physiological ecology. Annu Rev Physiol 68:253–278

Lingwood D, Simons K (2010) Lipids rafts as a membrane-organizing principle. Science 327:46–50

Loya Y, Sakai K, Yamazato K, Nakano Y, Sambali H, van Woesik R (2001) Coral bleaching: the winners and the losers. Ecol Lett 4: 122–131

Lu JZ, Hao YH, Chen JW (2001) Effect of cholesterol on the formation of an interdigitated gel phase in lysophosphatidylcholine and phosphatidylcholine binary mixtures. J Biochem 129:891–898

Mayfield AB, Hsiao YY, Fan TY, Chen CS, Gates RD (2010) Evaluating the temporal stability of stress-activated protein kinase and cytoskeleton gene expression in the Pacific reef corals *Pocillopora damicornis* and *Seriatopora hystrix*. J Exp Mar Biol Ecol 395: 215–222

Meesters EH, Bak RPM (1995) Age-related deterioration of a physiological function in the branching coral Acropora palmate. Mar Ecol Prog Ser 121:203–209

Meyer zu Heringdorf D, Jakobs KH (2007) Lysophospholipid receptors: signalling, pharmacology and regulation by lysophospholipid metabolism. Biochim Biophys Acta 1768:923–940

Murphy MP (2009) How mitochondria produce reactive oxygen species. Biochem J 417:1–13

Mykytczuka NCS, Trevorsb JT, Ferronic GD, Leduca LG (2011) Cytoplasmic membrane response to copper and nickel in *Acidithiobacillus ferrooxidans*. Microbiol Res 166:186–206

Okita M, Gaudette DC, Mills GB, Holub BJ (1997) Elevated level and altered fatty acid composition of plasma lysophosphatidylcholine (lysoPC) in ovarian cancer patients. Int J Cancer 71:31–34

Oku H, Yamashiro H, Onaga K, Iwasaki H, Takara K (2002) Lipid distribution in branching coral *Montipora digitata*. Fish Sci 68:517–522

Olbrich K, Rawicz W, Needham D, Evans E (2000) Water permeability and mechanical strength of polyunsaturated lipid bilayers. Biophys J 79:321–327

Ollila S, Hyvonen MT, Vattulainen I (2007) Polyunsaturation in lipid membranes: dynamic properties and lateral pressure profiles. J Phys Chem B 111:3139–3150

Pamplona R, Barja G, Portero-Otin M (2002) Membrane fatty acid unsaturation, protection against oxidative stress, and maximum life span. Ann NY Acad Sci 959:475–490

Pandey PR, Roy S (2011) Headgroup mediated water insertion into the DPPC bilayer: a molecular dynamics study. J Phys Chem B 115: 3155–3163

Rozentsvet OA, Nesterov VN, Sinyutina NF (2012) The effect of copper ions on the lipid composition of subcellular membranes in *Hydrilla verticillata*. Chemosphere 89:108–113

Sasaki Y, Asaoka Y, Nishizuka Y (1993) Potentiation of diacylglycerol-induced activation of protein kinase C by lysophospholipids. FEBS Lett 320:47–51

Sellmayer A, Danesch U, Weber PC (1996) Effects of different polyunsaturated fatty acids on growth-related early gene expression and cell growth. Lipids 31:S37–S40

Shier WT, Baldwin JH, Nilsen-Hamilton M, Hamilton RT, Thanassi NM (1976) Regulation of guanylate and adenylate cyclase activities by lysolecithin. Proc Natl Acad Sci U S A 73:1586–1590

Shoemaker SD, Vanderlick TK (2002) Stress-induced leakage from phospholipid vesicles: effect of membrane composition. Ind Eng Chem Res 41:324–329

Smith HL, Howland MC, Szmodis AW, Li Q, Daemen LL, Parikh AN, Majewski J (2009) Early stages of oxidative stress-induced membrane permeabilization: a neutron reflectometry study. J Am Chem Soc 131:3631–3638

Sohal RS, Orr WC (2012) The redox stress hypothesis of aging. Free Radic Biol Med 52:539–555

Soong K, Lang JC (1992) Reproductive integration in reef corals. Biol Bull 183:418–431

Stark G (2005) Functional consequences of oxidative membrane damage. J Membrane Biol 205:1–16

Szule JA, Fuller NL, Rand RP (2002) The effects of acyl chain length and saturation of diacylglycerols and phosphatidylcholines on membrane monolayer curvature. Biophys J 83:977–984

Tambutte S, Holcomb M, Ferrier-Pages C, Reynaud S, Tambutte E, Zoccola D, Allemand D (2011) Coral biomineralization: from the gene to the environment. J Exp Mar Biol Ecol 408:58–78

Tang CH, Tsao PN, Lin CY, Fang LS, Lee SH, Wang WH (2012) Phosphorylcholine-containing lipid molecular species profiling in biological tissue using a fast HPLC/QqQ-MS method. Anal Bioanal Chem 404:2949–2961

Tang CH, Lin CY, Lee SH, Wang WH (2014a) Cellular membrane accommodation of copper-induced oxidative conditions in the coral *Seriatopora caliendrum*. Aquat Toxicol 148:1–8

Tang CH, Fang LS, Fan TY, Wang LH, Lin CY, Lee SH, Wang WH (2014b) Cellular membrane accommodation to thermal oscillations in the coral *Seriatopora caliendrum*. PLoS ONE 9(8), e105345. doi: 10.1371/journal.pone.0105345

Trump BF, Berezesky IK (1996) The role of altered $[Ca^{2+}]_i$ regulation in apoptosis, oncosis, and necrosis. Biochim Biophys Acta 1313:173–178

van Meer G, Voelker DR, Feigenson GW (2008) Membrane lipids: where they are and how they behave. Nat Rev Mol Cell Biol 9:112–124

Vigh L, Escriba PV, Sonnleitner A, Sonnleitner M, Piotto S, Maresca B, Horvath I, Harwood JL (2005) The significance of lipid composition for membrane activity: new concepts and ways of assessing function. Prog Lipid Res 44:303–344

Yamashiro H, Oku H, Onaga K, Iwasaki H, Takara K (2001) Coral tumors store reduced level of lipids. J Exp Mar Biol Ecol 265:171–179

Yellowlees D, Rees TAV, Leggat W (2008) Metabolic interactions between algal symbionts and invertebrate hosts. Plant Cell Environ 31:679–694

Zehmer JK, Hazel JR (2005) Thermally induced changes in lipid composition of raft and non-raft regions of hepatocyte plasma membranes of rainbow trout. J Exp Biol 208:4283–4290